

HASPER: An Image Repository for Hand Shadow Puppet Recognition

Syed Rifat Raiyan[†] , Zibran Zarif Amio , and Sabbir Ahmed , Member, IEEE

Abstract—Hand shadow puppetry, also known as shadowgraphy or ombromanie, is a form of theatrical art and storytelling where hand shadows are projected onto flat surfaces to create illusions of living creatures. The skilled performers create these silhouettes by hand positioning, finger movements, and dexterous gestures to resemble shadows of animals and objects. Due to the lack of practitioners and a seismic shift in people’s entertainment standards, this art form is on the verge of extinction. To facilitate its preservation and proliferate it to a wider audience, we introduce HASPER, a novel dataset consisting of 8,340 images of hand shadow puppets across 11 classes extracted from both professional and amateur hand shadow puppeteer clips. We provide a detailed statistical analysis of the dataset and employ a range of pretrained image classification models to establish baselines. Our findings show a substantial performance superiority of traditional convolutional models over attention-based transformer architectures. We also find that lightweight models, such as MOBILENETV2, suited for mobile applications and embedded devices, perform comparatively well. We surmise that such low-latency architectures can be useful in developing ombromanie teaching tools, and we create a prototype application to explore this surmission. Keeping the best-performing model INCEPTIONV3 under the limelight, we conduct comprehensive feature-spatial, explainability, and error analyses to gain insights into its decision-making process. To the best of our knowledge, this is the first documented dataset and research endeavor to preserve this dying art for future generations, with computer vision approaches. Our code and data are publicly available.

Impact Statement—This research is an impetus towards utilizing AI tools to revitalize the hitherto underexplored cinematic art form of hand shadow puppetry. Such tools may help understand the creativity frontier in generative models, facilitate the development of applications to teach shadowgraphy, and unveil several prospects for entertainment. The existing works, though distally relevant to shadowgraphy, explore the digitization of such precursory art forms via approaches that have since been rendered primitive and obsolete. The novel dataset that we introduce in this paper, namely HASPER, consists of 8,340 diverse samples garnered from performance clips of variably skilled puppeteers. Our extensive benchmarking reveals that the task of classifying the puppet silhouettes is reasonably solvable

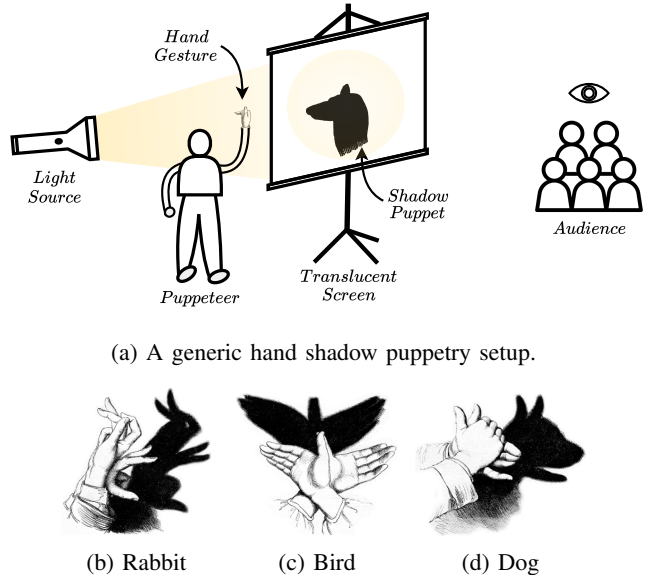
[†]Corresponding Author

This paper was submitted for review on 18 July 2024, at 08:25 AM Bangladesh Standard Time (UTC+06:00).

Syed Rifat Raiyan is affiliated with the Systems and Software Lab (SSL) of the Department of Computer Science and Engineering at the Islamic University of Technology, Boardbazar, Gazipur-1704, Dhaka, Bangladesh (e-mail: rifatraiyan@iut-dhaka.edu).

Zibran Zarif Amio, was affiliated with the Networking Research Group of the Department of Computer Science and Engineering at the Islamic University of Technology, Boardbazar, Gazipur-1704, Dhaka, Bangladesh. He is now with an AI-based software company, ReplyMind AI Ltd., Mirpur, Dhaka-1216, Bangladesh. (e-mail: zibranzarif@iut-dhaka.edu).

Sabbir Ahmed is affiliated with the Computer Vision Lab (CVLab) of the Department of Computer Science and Engineering at the Islamic University of Technology, Boardbazar, Gazipur-1704, Dhaka, Bangladesh (e-mail: sabbirahmed@iut-dhaka.edu).



(a) A generic hand shadow puppetry setup.



Fig. 1: Ombromanie in a nutshell².

using lightweight and convolutional feature extractor models, with accuracies of 88.97% by INCEPTIONV3 and 87.23% by MOBILENETV2. HASPER, as a data resource for all intents and purposes, can be a potential stride towards the preservation of this art form.

Index Terms—Hand shadow puppetry, benchmark, computer vision, dataset, deep learning, image classification, mobile application, ombromanie, shadowgraphy, silhouette, transfer learning

I. INTRODUCTION

Ombromanie, the ancient art of hand shadow puppetry, is a form of art that involves the mesmerizing interplay of light and shadow through the construction and manipulation of shadow figures or silhouettes on a surface, typically a screen or a wall, using one’s hands, body, or props [1]. The alias “*cinema in silhouette*”¹ is sometimes used to refer to this proto-cinematic medium of entertainment. Its working principle is very simple—the puppeteer adeptly positions their hands between a radiant light source and a translucent screen, consequently conjuring shadows and silhouettes that emulate different creatures [2] as shown in Figure 1. Despite its rich history and captivating allure across many cultures³, there

¹[https://en.wikipedia.org/wiki/Shadowgraphy_\(performing_art\)](https://en.wikipedia.org/wiki/Shadowgraphy_(performing_art))

²The shadowgraphy cliparts are adapted from ClipArt ETC, Florida Center for Instructional Technology, College of Education, University of South Florida. Link: <https://etc.usf.edu/clipart/galleries/266-hand-shadow-puppetry>

³<https://www.geniimagazine.com/wiki/index.php/Shadowgraphy>

exists a notable dearth of resources specifically tailored to this artistic domain. With properly annotated and sourced data, researchers could study the intricacies of hand silhouette movements, shapes, and storytelling techniques, thereby enabling the development of sophisticated Artificial Intelligence (AI) systems for automatic recognition, classification, or even generation of ombromanie performances [3]. The generation aspect is particularly relevant given the demonstrable impotency of AI image generator models in accurately creating hands and fingers [4]. Apart from that, the development of applications that can facilitate the learning of ombromanie has the potential to breathe new life into this waning art form [5]. In 2011, UNESCO recognized shadow puppetry as an endangered artistic tradition by adding it to the Intangible Cultural Heritage list [6], which is why it necessitates more preservatory apparatus and research efforts.

In tandem with this motivation, this work introduces a seminal addition to the realm of data resources, HASPER (**H**and **S**hadow **P**uppet **I**mage **R**epository), a methodically curated novel image dataset of hand shadow puppets. The dataset comprises an assemblage of 8,340 samples, that we painstakingly source and verify from 45 professional puppeteer clips and 22 amateur puppeteer clips. We label and categorize the images with utmost precision to elicit robustness in the image classification models that will undergo training with these images. The samples in HASPER are diverse in nature since the source clips are recorded in a plethora of different poses, orientations, and background lighting conditions of the translucent screen. We conduct a detailed analysis of HASPER's statistical characteristics. We also employ a variety of state-of-the-art (SOTA) pretrained image classification models to establish a performance benchmark for validating the integrity of the dataset. Additionally, we conduct a thorough evaluation of several facets of the ace INCEPTIONV3 model, including its feature representations, interpretability, explainability, and classification errors that it encounters. In an effort to assess the potential of digitized ombromanie teaching tools, we create a simple and lightweight prototype Android application using Flutter for classifying hand shadow puppet images from the phone's camera feed. We posit that our dataset possesses the potential to offer a wealth of opportunities for exploration and analysis into the artistic domain of hand shadow puppetry.

II. LITERATURE REVIEW

The recognition and classification of hand shadow puppet images are intriguing problems in the context of deep learning, albeit relatively underexplored. After rigorously analyzing the existing pool of research on the topic, we could identify several quasi-related works.

A. Image Classification and Recognition

Among the pioneering endeavors in hand shadow image classification was that of Huang et al. [7], who created SHADOW VISION—a system to emulate an immersive virtual shadow puppet theater experience, employing a user's hand gestures over an overhead projector to control the creation

and manipulation of objects within a 3D Open Inventor⁴ environment. The chain of stages underlying the implementation of SHADOW VISION were acquisition, segmentation, feature extraction, and recognition of the infrared shadow puppet images. They also adopted a 3-layer neural network and the centralized contour moments modeling technique, using 13 features (7 moments of the object, length, angle, and the 4 endpoints of the axis of inertia). The data used for this study isn't publicly available, and the methodology can be deemed somewhat obsolete in the modern purview, due to being supplanted by the emergence of deep learning models.

Some recent works explore different convolutional models to assess their efficacy in Indonesian shadow puppet recognition. Sudiatmika et al. [8], Sudiatmika and Dewi [9] used the deep CNN models, ALEXNET [10] and VGG-16 [11], and constructed a dataset of 2,530 images spanning 6 classes of puppets from museums in Bali. They also experimented with other convolutional models, such as MASK R-CNN [12] and MOBILENET [13], in two separate studies [14, 15].

In a similar spirit, our work is an endeavor towards establishing a performance benchmark of the recent SOTA feature extractor models for hand shadow puppet contour images, in a more large-scale and comprehensive manner.

B. 3D Modeling and Human Motion Capture

One of the earliest works involving silhouettes is a study by Brand [16] that explored the mapping of monocular monochromatic 2D shadow image sequences of humans to animated 3D body poses, using a configural and dynamical manifold created from data with a topologically special hidden Markov model (HMM), acquired via the process of entropy minimization without resorting to any articulatory body model. Several advances in vision-based human motion capture and analysis since then have leveraged human silhouette templates [17, 18], more specifically, hand and finger silhouettes [19, 20, 21].

C. Robotics

Huang et al. [22] introduced computer vision-aided shadow puppetry with robotics by matching shape correspondences of input images. They claimed that due to the physical limitations of human arms, it is often not feasible to construct complex shadow forms. Instead, they developed a framework that enabled them to produce shadow images with the mechanical arms of a robot. The authors built a library of shadow images and used them to orient the robotic arms into a formation resembling the intended shadow puppet. The data used for this study isn't publicly available.

D. Human-Computer Interaction

The authors of [23] proposed a framework for controlling two Chinese shadow puppets—a human model and an animal model, with the use of body gestures via a Microsoft Kinect sensor. Carr and Brown [24] conducted a similar work by building a real-time Indonesian shadow puppet storytelling application that is capable of mimicking the full-body actions of the user, using the Microsoft Kinect sensor. In order to

⁴Open Inventor™ toolkit — <https://www.openinventor.com/>

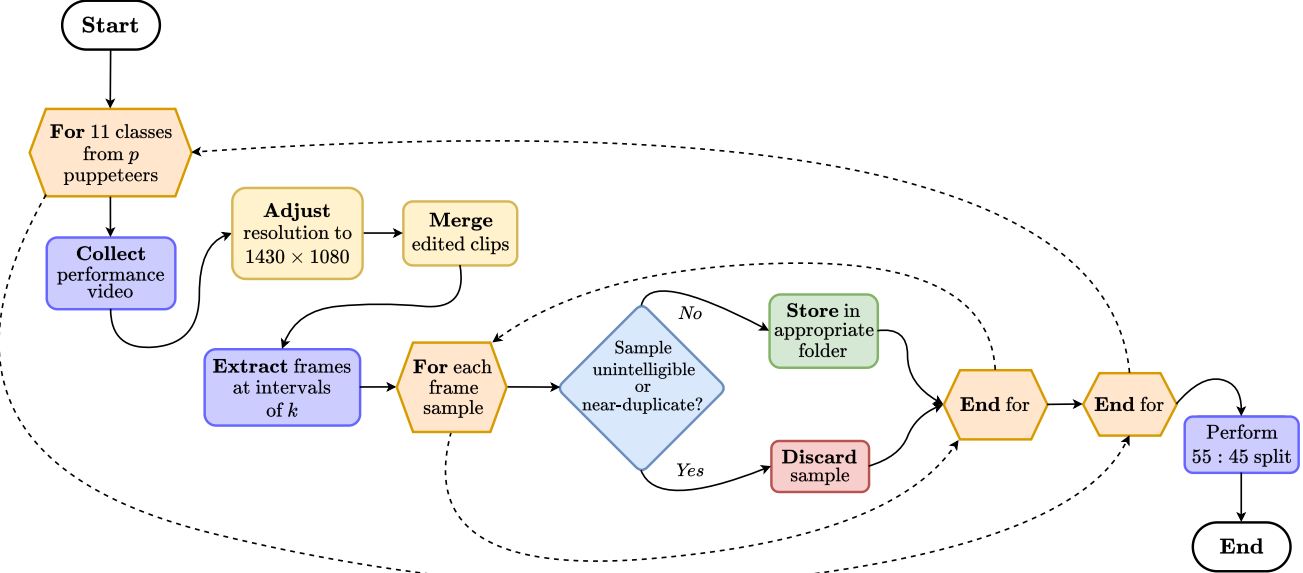


Fig. 2: A flowchart depicting the dataset construction process.

leverage contactless gesture recognition (CGR) to teach traditional Chinese shadow puppetry to beginners, Tsai and Lee [25] developed a system using Leap Motion sensors. These studies on digitizing the art of shadow puppetry, or puppetry in general, were influenced to some extent by other similar works in the gesture recognition domain [26, 27, 6, 28, 29, 30]. Tang *et al.* [31] developed an intelligent shadow play system, called SHADOWTOUCH, which includes a multidimensional somatosensory interaction module coupled with an automatic choreography module, to facilitate natural interaction between the shadow play figures and the human users.

The motif of our work tessellates well with the core objectives of the aforementioned research works. The utilization of digitized traditional arts serves as a means to preserve their inherent legacies, and HASPER can be a potent contribution to the contemporary pool of resources to facilitate such innovative digitization for ombromanie.

III. DATASET CONSTRUCTION

The series of steps involved in our data acquisition process is broadly divided into three tasks — (a) procuring the performance clips, (b) extraction of the frames, and (c) categorization of each sample frame with a proper label. Figure 2 portrays this workflow behind our dataset preparation. We incorporate manual oversight at each step of the dataset creation in order to reconcile any exigencies pertaining to the quality of HASPER.

A. Collating Shadowgraphy Clips

At the outset of the process, we procure 45 different clips of 9 different professional shadowgraphists from YouTube⁵. The video sources are licensed under fair use and a list consisting of the links to all of them is available in our GitHub⁶.

TABLE I: Statistical summary of HASPER.

Silhouette Class	Clips		Sample Distribution		
	Pro.	Nov.	Training	Validation	Total
Bird	6	2	447	361	808
Chicken	2	2	431	389	820
Cow	2	2	412	223	635
Crab	4	2	367	328	695
Deer	6	2	423	379	802
Dog	7	2	466	365	831
Elephant	5	2	420	315	735
Moose	3	2	394	322	716
Panther	2	2	367	396	763
Rabbit	4	2	415	348	763
Snail	4	2	461	311	772
Total	45	22	4603	3737	8340
		67			

repository. We record the relevant portions of the performance videos using the open-source recording software OBS Studio⁷. Two novice volunteer shadowgraphists collectively produce 22 additional clips, with each contributing one clip for every class. As a consequence, the total number of source clips aggregates to $45 + (11 \times 2) = 67$.

B. Extracting Samples

To mitigate the presence of excessively similar and redundant image samples, we extract frames from these clips at reasonable intervals of k after downscaling the clips to a resolution of 1430×1080 . The values of k are judiciously chosen for the clips of each class, and every k th frame is selected as a candidate image sample (*e.g.*, with $k \approx 180, 200, 220$ for a 60 FPS clip). Table I encapsulates some essential

⁵<https://www.youtube.com>

⁶GitHub repository — <https://github.com/Starscream-11813/HaSPeR>

⁷Open Broadcaster Software® — <https://obsproject.com/>

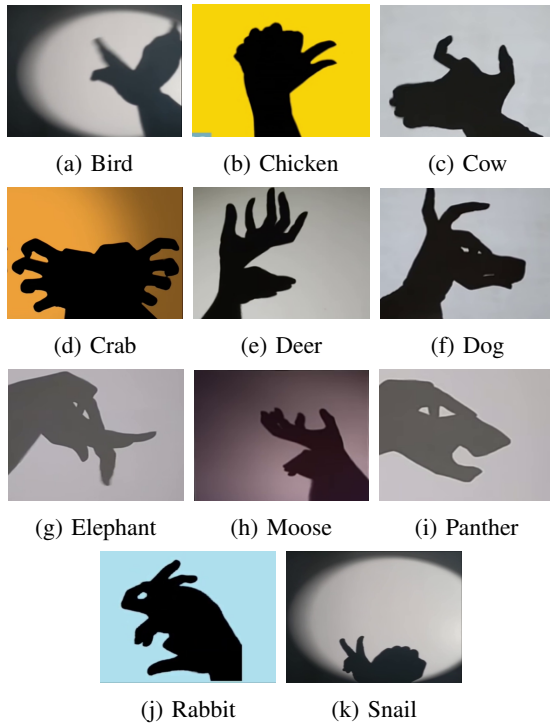


Fig. 3: Samples from each class of the dataset.

statistical information related to HASPER and provides a superficial overview of the dataset.

C. Labeling

After the extraction of the frames, the samples undergo manual scrutiny by 3 annotators who are pursuing undergraduate studies in Computer Science and Engineering (CSE). If a series of contiguous samples *prima facie* exhibit substantial similarity, we only keep a single image from that set of samples. The rest are discarded to avoid redundancy and to instill diversity. Another criterion that dictates the legitimacy of an image sample is its intelligibility. If the majority of the annotators agree on the unintelligibility of a sample, they discard it in unison. After performing this omission of unsuitable samples for each class, we end up with 11 different directories of images, each containing the curated samples of a particular class. The images in these folders are then further partitioned into training and validation sets, maintaining a 55:45 split approximately. We also pragmatically incorporate a proper distribution of the samples sourced from amateur clips over both the training and validation sets, to avoid making the latter unfairly difficult for the classification models.

IV. DATASET DESCRIPTION

To provide a tangible exposition of the diverse samples in the dataset, Figure 3 presents a collection of representative images across all the 11 classes. With minimally astute perspicacity, we can observe that the samples vary in terms of the nature of the backgrounds, the anatomical structure of the puppeteers' hands, the photometric opacity and sharpness of the projected silhouettes, and a panoply of other aspects.

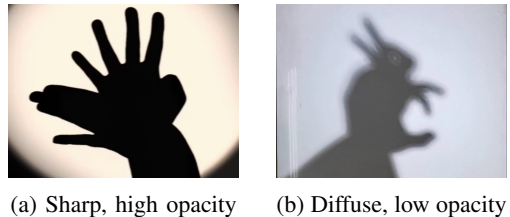


Fig. 4: Samples with different silhouette properties.

A. Background Variance

The hand shadow puppetry setup that a puppeteer's crew arranges before the performance greatly dictates the nature of the background on which the shadow puppets are displayed. If the location of the light source is very near to the wall or the translucent screen, then we can observe an elliptical shadow contour on the background as evident in Figures 3a and 3k. The angular directionality of the light also manifests a gradient effect on the background as can be seen in Figures 3d and 3h. The temperature and color of the light emanated by the light sources onto the screens also add to the diversity.

B. Nature of the Silhouettes

The positioning of the light source with respect to the puppeteer's hands plays a role in shaping the shadows' quality. Proximity to the light source yields crisp, well-defined shadows (*e.g.*, Figure 4a), while increasing the distance fosters softer, more diffuse shadows (*e.g.*, Figure 4b) with a central umbra and peripheral penumbra. The higher the contrast between the silhouettes and their respective backdrops, the more visible and well-contoured the shadow puppets are. The direction of the light source influences the orientation and shape of the shadows. Shadows cast by overhead lighting sources may appear elongated, while shadows cast by low-angle lighting sources may exhibit softer edges and less pronounced contrast and sharpness. The shadows also differ in terms of the magnitude of their opacity, *i.e.*, the degree to which the hands prevent the transmission of light being projected onto the screen.

C. Hand Anatomy and Stylistic Flair of the Puppeteers

The physiological properties of the puppeteers' hands can vary significantly due to a combination of genetic factors, environmental influences, and lifestyle choices. These nuanced



Fig. 5: 'Deer' samples with different artistic representations.

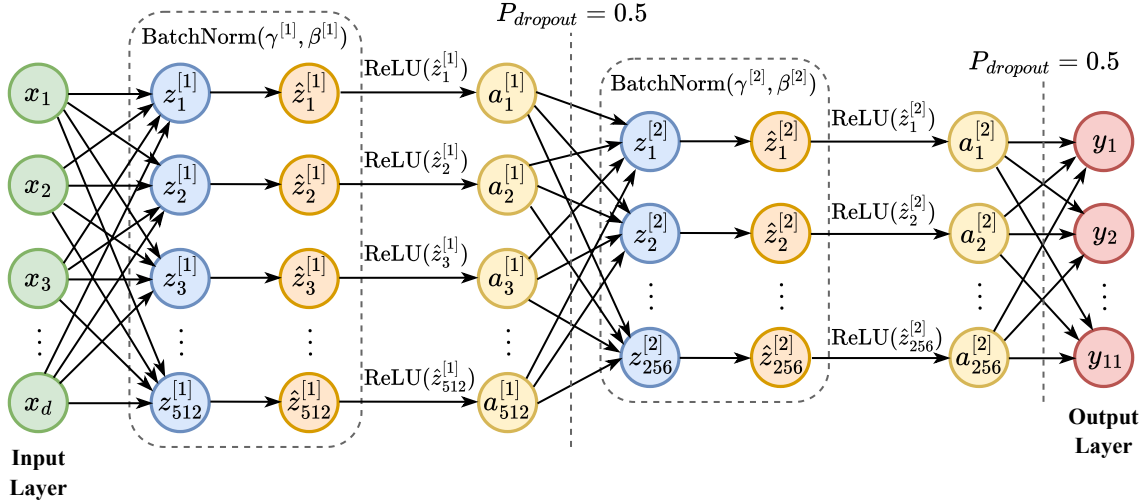


Fig. 6: Classifier block attached to the tail-end of the pretrained models. Here, d is the feature dimension of the anterior pretrained image classification model. The output features of layer l is $z^{[l]} = W^{[l]}a^{[l-1]}$, where $a^{[l-1]}$ denotes the activation values of the preceding $(l-1)$ th layer. The batch normalized value of the i th output feature $z_i^{[l]}$ is $\hat{z}_i^{[l]} = \gamma^{[l]}z_{norm}^{[l]} + \beta^{[l]}$, where γ and β are learnable parameters. The activation values of layer l are denoted by $a^{[l]} = g(\hat{z}^{[l]})$ which is computed using the activation function $g = \text{ReLU}$.

anatomical variations of the wrists, palms, and digits of the puppeteers, along with the different stylistic choices they employ in their choreography, contribute as yet another avenue of diversity of the image samples in HASPER. Figure 5 pristinely demonstrates the morphological variations of hand shadow puppets belonging to the ‘Deer’ class.

D. Comparative Analysis

1) Inter-class Similarity

Due to the conspicuous resemblance in the anatomical structures of certain animal species, the samples belonging to the classes corresponding to those animals exhibit a notable degree of similarity as well. Figures 3e and 3h are prime examples of such structural similitude that can be observed between the ‘Deer’ and ‘Moose’ classes. These similarities make the image classification task on HASPER quite challenging and culminate to being the reason behind a lot of misclassifications, as discussed in Section V-C.

2) Intra-class Dissimilarity

Some classes include samples of multiple species of the same animal, and these samples are starkly different in appearance from one another. Given the presence of such quasi-disparate samples, along with the individualistic flair that manifests through the puppeteers’ stylistic choices, a particular class may show a lot of intra-class dissimilarity. As aforementioned, Figure 5 portrays the heterogeneity of this nature among the samples from the ‘Deer’ class.

E. Statistical Analysis

Table I presents the statistical properties of the HASPER dataset. It tabulates the proportion of samples belonging to each of the 11 classes and their corresponding training-validation splits. The ‘Dog’ class has the highest number of images (831 samples $\approx 9.96\%$), while on the contrary,

the ‘Cow’ class possesses the least number of images (635 samples $\approx 7.61\%$). This suggests that overall, hand shadow puppetry of dogs is the most popular—a fact that concurs well with our anecdotal observations while searching for hand shadow puppetry performances. The proportions of samples belonging to the ‘Crab’, ‘Elephant’, and ‘Moose’ classes (8.33%, 8.81%, and 8.59% respectively) are also slightly low due to a scarcity of performance clips starring hand shadow puppets of these classes. As evident in Table I, the image samples are quite evenly distributed across all 11 classes. Each class has $\approx 66.72 \pm 0.36\%$ samples sourced from clips of professional performers and the rest $\approx 33.27 \pm 0.58\%$ samples sourced from amateur clips. In totality, we end up with 4,603 samples in the training set and 3,737 samples in the validation set, thereby partitioning HASPER following a 55:45 ratio.

V. DEVELOPING BENCHMARK FOR HASPER

A series of pretrained models are used as feature extractors to develop a benchmark for the dataset. The models are pretrained on the IMAGENET [51] dataset and fine-tuned on HASPER. We implement the training pipeline using the Pytorch⁸ framework. This section presents an overview of the models, evaluation metrics, and experimental results.

A. Experimental Setup

1) Baseline Models

For this classification task, we use 31 feature extractor models as baselines, which are listed in Table II. Some of these models have a track record of good performance across various other image classification tasks [52]. We examine both conventional Convolutional Neural Networks (CNNs) and CNNs augmented with attention mechanisms. Some models have

⁸<https://pytorch.org/vision/stable/models.html>

TABLE II: Performance comparison of the vanilla and modified versions of the image classification models.

Models	Params.	Performance Metrics											
		Vanilla						w/ Classifier Block					
		Top- k Accuracy (%)			Precision	Recall	F1-score	Top- k Accuracy (%)			Precision	Recall	F1-score
		Top-1	Top-2	Top-3				Top-1	Top-2	Top-3			
SHUFFLENETV2X10 [32]	2.3M	46.29	60.71	72.97	0.6006	0.4576	0.4225	81.64	87.26	92.23	0.8405	0.823	0.7989
ViTB16 [33]	86.6M	65.9	75.06	79.82	0.7214	0.6649	0.6462	59	68.15	73.72	0.6576	0.5965	0.5792
ViTL32 [33]	306.5M	75.94	82.82	89.08	0.7998	0.7716	0.7443	77.89	85.14	90.5	0.8158	0.7891	0.7614
ALEXNET [10]	61.1M	79.04	84.05	88.19	0.826	0.8015	0.7718	81.85	88.41	92.05	0.8448	0.8261	0.8022
SQUEEZENET1_1 [34]	1.2M	80.67	85.57	88.94	0.83	0.8127	0.7912	80.35	85.68	89.77	0.8296	0.8135	0.7902
MOBILENETV3SMALL [35]	2.5M	81.08	86.13	92.18	0.8529	0.8221	0.7993	81.72	87.1	90.98	0.8513	0.8258	0.8012
CONVNEXTLARGE [36]	197.8M	81.58	87.53	91.78	0.8441	0.8208	0.7997	84.93	88.86	92.9	0.8783	0.8522	0.8384
EFFICIENTNETB0 [37]	5.3M	81.91	85.38	90.42	0.8625	0.829	0.8012	83.54	88.22	92.96	0.8611	0.8418	0.8231
WIDERESNET50_2 [38]	68.9M	83.32	88.76	95.53	0.8596	0.8416	0.8158	85.65	91.06	94.32	0.8751	0.861	0.8444
MNASNET13 [39]	6.3M	83.43	86.35	88.94	0.8495	0.8388	0.8173	82.57	88.28	92.58	0.8445	0.8315	0.8094
VGG16 [11]	138.4M	83.48	87.87	91.94	0.8462	0.8376	0.8187	84.85	90.95	94.4	0.857	0.8516	0.8364
VGG19 [11]	143.7M	83.97	90.07	93.57	0.8636	0.8449	0.8307	84.02	90.09	93.25	0.8623	0.8401	0.8274
MOBILENETV3LARGE [35]	5.5M	84.23	90.71	94.86	0.8727	0.8468	0.83	83.32	87.79	93.57	0.8682	0.842	0.8218
EFFICIENTNETV2S [40]	21.5M	84.72	89.24	92.15	0.8667	0.8523	0.8329	85.97	90.01	92.26	0.876	0.8628	0.8482
MOBILENETV2 [41]	3.5M	84.8	90.28	94.88	0.8742	0.8563	0.8373	87.23	92.32	94.48	0.8837	0.8774	0.8668
GOOGLENET [42]	6.6M	84.93	90.12	93.84	0.8615	0.8541	0.8348	83.97	88.97	92.4	0.8554	0.8448	0.8244
SWINV2B [43]	87.9M	84.98	89.96	94.11	0.8747	0.8551	0.8439	81.34	86.88	93.22	0.853	0.8227	0.8021
CONVNEXT [36]	88.6M	85.17	89.8	95.34	0.8751	0.856	0.8431	86.75	91.03	94.46	0.8803	0.8728	0.8608
RESNET18 [44]	11.7M	85.36	92.56	94.4	0.8807	0.863	0.8411	85.84	92.61	95.21	0.8793	0.8665	0.8494
SWINB [45]	87.8M	85.84	92.72	97.35	0.8789	0.8643	0.8535	85.12	91.67	95.23	0.8772	0.8564	0.843
RESNET101 [44]	44.5M	86.37	93.17	95.85	0.8837	0.8706	0.8508	86.54	93.97	97	0.8764	0.8719	0.8556
MAXViT [46]	30.9M	86.54	93.84	97.05	0.8903	0.8691	0.8642	85.2	91.54	95.18	0.8722	0.857	0.847
REGNETX32GF [47]	107.8M	86.67	91.14	95.63	0.8879	0.8735	0.857	86.99	92.13	95.21	0.8823	0.8742	0.8608
DENSENET201 [48]	20.0M	86.83	90.23	92.74	0.8853	0.8701	0.8548	88.89	93.49	95.42	0.9042	0.8953	0.8844
RESNET152 [44]	60.2M	86.86	90.42	94.4	0.8929	0.877	0.8585	86.64	91.57	94.51	0.8844	0.8715	0.8576
RESNET50 [44]	25.6M	86.91	92.74	95.47	0.8953	0.8771	0.8607	84.69	90.12	94.08	0.8717	0.8538	0.8357
RESNET34 [44]	21.8M	87.55	92.93	95.55	0.8943	0.8809	0.8699	85.79	91.73	93.79	0.8767	0.8634	0.8461
WIDERESNET101_2 [38]	126.9M	87.77	92.37	95.1	0.8955	0.8833	0.8684	86.27	92.45	96.14	0.8783	0.869	0.8533
DENSENET121 [48]	8.0M	87.9	92.4	94.75	0.8947	0.8844	0.8719	86.08	90.95	94.64	0.8771	0.866	0.8498
RESNEXT101_32X8D [49]	88.8M	88.62	93.17	95.85	0.9045	0.8927	0.8803	86.54	93.97	97	0.9073	0.896	0.8839
INCEPTIONV3 [50]	27.2M	88.97	92.77	94.19	0.8979	0.8943	0.8828	88.3	92.29	95.34	0.8905	0.8849	0.8777

multiple variants in terms of size or number of parameters, and we compare the performance among those variants as well.

2) Performance Metrics

We use top- k validation accuracy values (with $k = 1, 2, 3$), Precision, Recall, and F1-score as evaluation metrics to perform comparative analyses among the aforementioned models. The latter three judgment criteria are used due to the slightly imbalanced nature of HASPER, as evident in Table I.

3) Classifier Network

We adopt two approaches to arrive at the final 11-dimensional layer since there are a total of 11 classes to predict from. The first approach is to directly append an 11-dimensional fully connected layer at the tail-end of the vanilla models. The second approach incorporates the classifier block portrayed in Figure 6.

4) Hyperparameters and Optimizer

We use Stochastic Gradient Descent (SGD) [53], with a learning rate $\alpha = 0.001$ and momentum $\gamma = 0.9$, as the optimizing method, and Cross Entropy Loss as the loss metric for all the models. To decay the learning rate, we use Step Scheduler, which decays α by 0.1 every 5 epochs. Each model undergoes training for 50 epochs to ensure equitable compari-

son, and we empirically ascertain that 50 epochs are sufficient for the majority of the models to achieve convergence.

5) Data Augmentation and Preprocessing

In order to generate a more diverse pool of training samples, we also incorporate data transformation techniques⁹—Random Resize, Random Perspective, Color Jitter, Random Horizontal Flip, Random Crop, Random Rotation, Gaussian Blur, and Random Affine with translation and shearing—while training the models. We choose these data augmentation techniques since the classes in HASPER are mostly rotationally asymmetric and incongruent. Consequently, the augmented samples aid in eliciting better generalization abilities and robustness for all the models. The input images that are fed to the models are appropriately resized *a priori* using Bicubic Interpolation.

B. Results and Findings

1) Performance Analysis

The INCEPTIONV3 model yielded the best performance with a top-1 accuracy of 88.97%. The vanilla version of the model also yields reasonably high Precision, Recall,

⁹<https://pytorch.org/vision/stable/transforms.html>

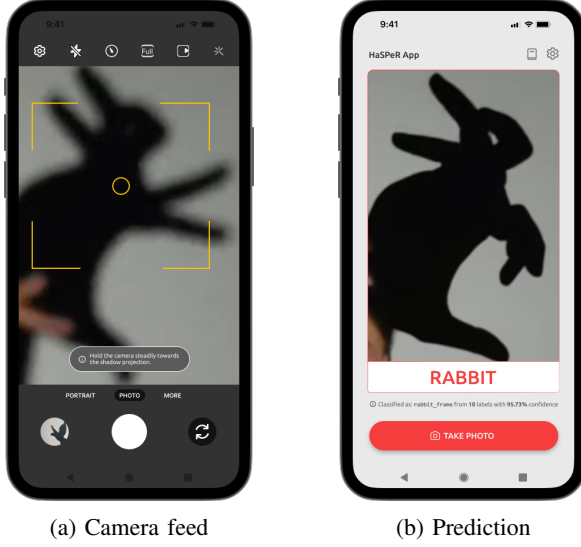
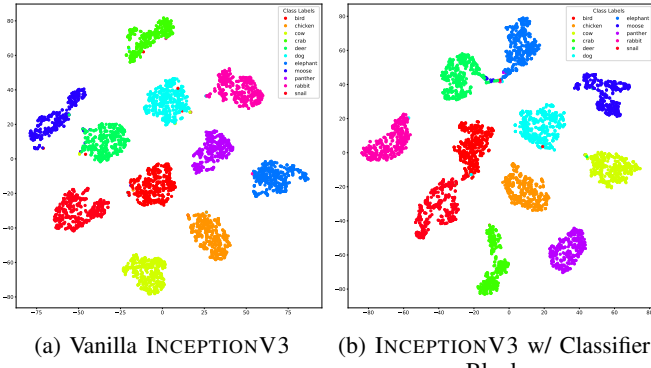


Fig. 7: Android application for shadow puppet recognition.

and F1-score of 0.8979, 0.8943, and 0.8828 respectively. In terms of top-2 and top-3 accuracy values, we observe the competence of transformer architectures like SWINB and MAXViT, with each achieving the highest top-2 and top-3 accuracy scores, respectively. Upon being equipped with the classifier block shown in Figure 6, the DENSENET201 model yields the highest top-1 accuracy and F1-score. In contrast, the RESNEXT101_32X8D model demonstrates the best performance across all the other evaluation metrics. At this recess of the performance analysis, we consider the top-1 accuracy metric to be the most statistically significant metric. As evident in Table II, the RESNEXT101_32X8D model lags behind the INCEPTIONV3 model when it comes to the top-1 accuracy value in both cases, which is why we adjudicate that the latter is the best-performing model. It is noteworthy to point out that MOBILENETV2, with only 3.5 million parameters, managed to surpass many of the other models in terms of performance. This indicates the suitability of this image classification task for lighter, low-latency models that can be used in mobile applications and embedded devices. We create a simple prototype Android application using Flutter

Fig. 8: *t*-Distributed Stochastic Neighbor Embedding (*t*-SNE) feature representations of INCEPTIONV3.

to test the efficacy of MOBILENETV2 in classifying hand shadow puppet images from the phone’s camera feed. Figure 7 portrays the snapshots of the prototype application.

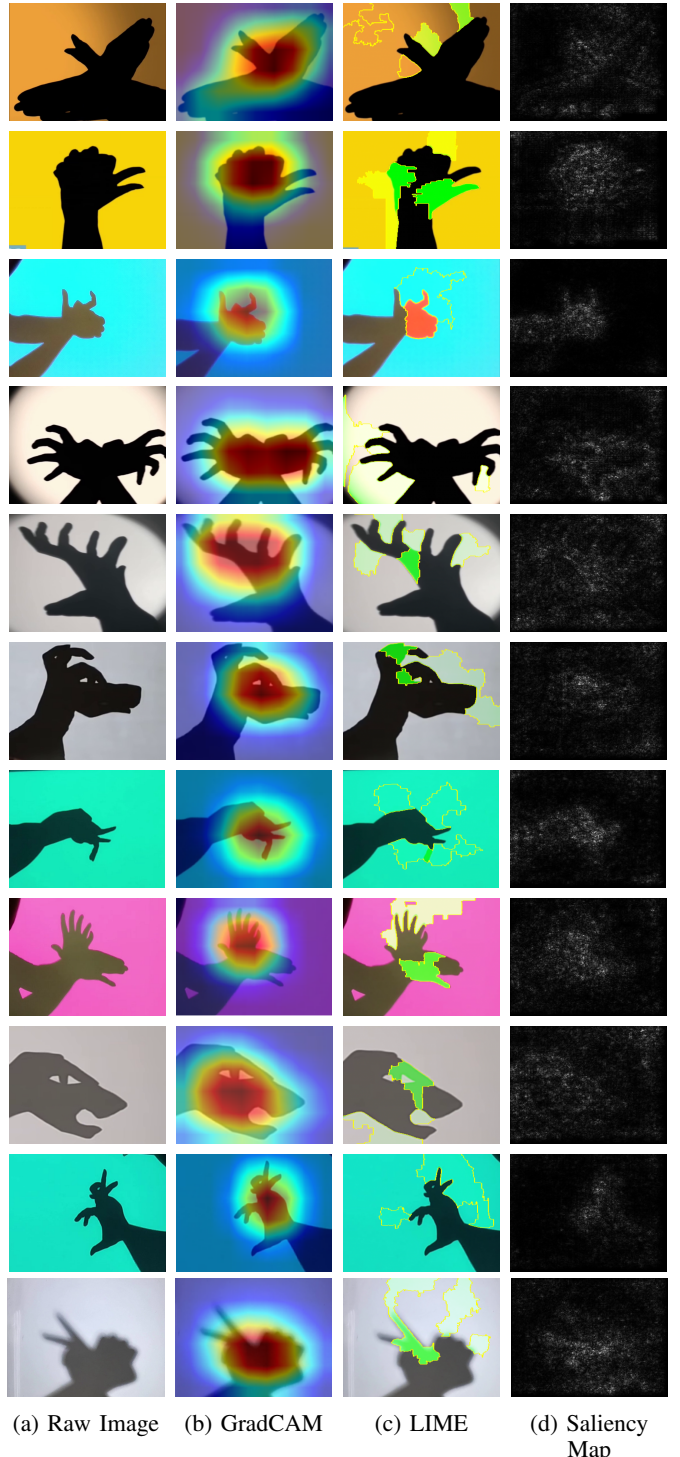


Fig. 9: The juxtaposition of original image samples from the HASPER dataset with their corresponding GradCAM Heatmaps, LIME Visualizations, and Saliency Maps (for the best-performing vanilla INCEPTIONV3 model).

2) Feature Space Visualization and Analysis

In order to visualize the learned feature space of INCEPTIONV3, we resort to the dimensionality reduction technique

called *t*-Distributed Stochastic Neighbor Embedding [54] since it can preserve the proximity of high-dimensional data points. For high-dimensional data residing on or proximate to a low-dimensional, non-linear manifold, it becomes imperative to preserve this proximity of the collapsed low-dimensional representations for closely resembling data points. Achieving such proximity preservation is often unattainable through linear mappings such as Principal Component Analysis (PCA), which is why we opt for the *t*-SNE dimensionality reduction approach. We can pragmatically infer from the 2D-collapsed visualizations of the high-dimensional feature representations in Figure 8, that the classes are nicely clustered and congealed with minimal overlaps and outliers. This enables the model to easily determine the decision surface in the high-dimensional feature space and perform very well on the classification task.

3) Qualitative Analysis and Explainability

As depicted in Figure 9, we adopt a plethora of Explainable AI (xAI) techniques for the best-performing INCEPTIONV3 model to understand its decision-making. While viewing the GradCAM (Gradient-weighted Class Activation Mapping) [55] attention heatmaps, it becomes apparent that the model puts more gravitas on the common-sense distinguishing traits. For example, in Figure 9b, we observe the regions of the image samples predominantly influencing their respective classification scores—the wingspan and beak of a bird, the gallinaceous comb of a chicken, the horns and concave head of a cow, the appendages of a crab, the horns of a deer, the long-slanted head of a dog, the tusks of an elephant, the upright horns of a moose, the big eyes and small ears of a panther, the petite hands and head of a rabbit, as well as the shell and antennae of a snail. As human beings, we evoke these same distinguishing characteristics while classifying the images using our own visual reasoning faculties. As exemplified in Figure 9c, for local interpretation, we use the model-agnostic technique called LIME (Local Interpretable Model-agnostic Explanations) [56]. We also demonstrate the spatial support of the top-1 predicted

True Labels		Predicted Labels										
		Bird	Chicken	Cow	Crab	Deer	Dog	Elephant	Moose	Panther	Rabbit	Snail
Bird	279	6	27	0	3	8	0	9	0	0	29	
Chicken	1	388	0	0	0	0	0	0	0	0	0	0
Cow	1	4	215	0	0	1	0	0	0	0	0	2
Crab	24	12	0	178	6	0	0	44	0	62	2	
Deer	1	1	11	0	365	0	0	1	0	0	0	
Dog	3	0	0	0	0	361	0	0	1	0	0	
Elephant	0	0	0	0	0	0	315	0	0	0	0	
Moose	1	0	0	0	1	0	0	320	0	0	0	
Panther	7	0	0	0	0	29	107	0	253	0	0	
Rabbit	0	0	0	1	0	0	0	0	1	345	0	1
Snail	0	2	0	0	0	3	0	0	0	0	306	

Fig. 11: Confusion Matrix of vanilla INCEPTIONV3.

classes by generating the saliency maps [57] in Figure 9d. These maps are rendered using a solitary back-propagation pass through the INCEPTIONV3 model, and they accentuate the salient areas of the given image, characterized by their discriminative attributes with respect to the given class.

C. Error Analysis

The confusion matrix for the INCEPTIONV3 model on our dataset, presented in Figure 11, reveals that the ‘Panther’ class exhibits the highest count of misclassifications. One obvious reason for this is the somewhat significant inter-class similarity among the ‘Dog’, ‘Elephant’, and ‘Panther’ classes. Most of the misclassified samples are from visually similar classes. We can posit that navigating the intricacies of visually similar classes poses a significant challenge in this image classification task, as evident from the other pale-red entries of the confusion matrix in Figure 11. Even to the keen human eye, distinguishing between these classes may be perplexing, as they share common visual features, shapes, or color patterns that result in a high degree of resemblance. We examine various aspects, such as the distinctive features or characteristics that might have led to confusion and the degree of similarity between the misclassified classes. Figure 10a and 10b show the confusion between a ‘Crab’ sample and a ‘Rabbit’ sample which look visually quite similar. The same holds for the sole ‘Moose’ sample that is misclassified as a ‘Bird’ sample by the INCEPTIONV3 model, as depicted in Figure 10c and 10d. We observe that misclassifications of this type occur when images belonging to different, but visually akin categories, are erroneously assigned to the wrong class. The green entries along the diagonal of the confusion matrix in Figure 11 indicate the reasonably good classwise prediction performance of the INCEPTIONV3 model, even though there exists a slight class imbalance in HASPER.

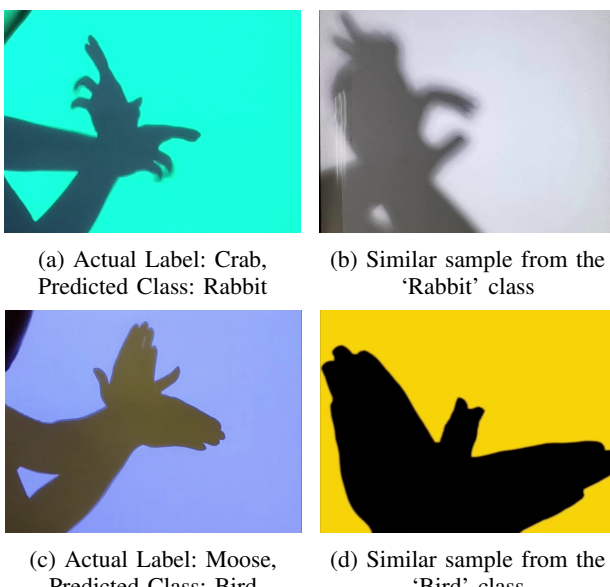


Fig. 10: Misclassified samples with visually similar samples of the predicted class.

VI. CONCLUSION AND FUTURE WORK

In this paper, we explore an intriguing subject matter, hand shadow puppetry, in the realm of computer vision. We introduce HASPER, a novel dataset with a sizable collection of 8,340 hand shadow puppet images distributed across 11 classes, taken from both expert and amateur puppetry performance clips. We fine-tune 31 pretrained image classification models on HASPER to establish a benchmark for the dataset. To explain and analyze the performance of the most erudite model, INCEPTIONV3, in comparison with other baseline models, we visually manifest its feature space using the *t*-SNE dimensionality reduction technique. We also perform thorough qualitative and error analyses for the INCEPTIONV3 model. We envisage the possibility of developing applications for imparting the art of shadowgraphy, via mobile and embedded devices. We claim that this work is novel and significant since it is the first publicly available dataset and study on image classification benchmarking that focuses only on ombromanie. There are many avenues in our work that warrant further investigation. We hope to reconcile those desiderata by enriching our dataset with numerous permutations of arm positions and finger movements, preferably by employing more skilled individuals with varying palm and wrist structures, thereby creating more diverse silhouettes. We stipulate that the dataset, in a more supplemented state, will be better suited to fine-tune models with a very large number of parameters. We also plan to experiment with a gesture detection technology such as MediaPipe¹⁰ or Microsoft Kinect¹¹ for leveraging depth coordinates of hand landmarks [58], and assess their efficacy in classifying hand shadow puppets.

VII. ACKNOWLEDGMENTS

We convey our heartfelt gratitude, in advance, to the anonymous reviewers for their constructive criticisms and insightful feedback which will surely be conducive to the improvement of the research work outlined in this paper. We also appreciate the Systems and Software Lab (SSL) of the Islamic University of Technology (IUT) for the generous provision of computing resources during the course of this project. Additionally, we wish to acknowledge Shahriar Ivan, Department of Computer Science and Engineering, Islamic University of Technology, for his invaluable assistance in proofreading and offering a preliminary review of this manuscript. Syed Rifat Raiyan, in particular, wants to thank his parents, Syed Sirajul Islam and Kazi Shahana Begum, for everything.

REFERENCES

- [1] A. Almoznino and Y. Pinas, *The art of hand shadows*. Courier Corporation, 2002.
- [2] E. T. Clearinghouse, “Hand shadow puppetry gallery,” <https://etc.usf.edu/clipart/galleries/266-hand-shadow-puppetry>, Florida Center for Instructional Technology, College of Education, University of South Florida, 2004, accessed: 2024.
- [3] A.-S. Maerten and D. Soydaner, “From paintbrush to pixel: A review of deep neural networks in ai-generated art,” *arXiv preprint arXiv:2302.10913*, 2023.
- [4] D. Samuel, R. Ben-Ari, S. Raviv, N. Darshan, and G. Chechik, “Generating images of rare concepts using pre-trained diffusion models,” in *Proceedings of the AAAI*, vol. 38, no. 5, 2024, pp. 4695–4703.
- [5] R. Saritha, “An artist nurturing a dying art and his quest for its conservation,” *YourStory*, 2017.
- [6] F. Lu, F. Tian, Y. Jiang, X. Cao, W. Luo, G. Li, X. Zhang, G. Dai, and H. Wang, “Shadowstory: creative and collaborative digital storytelling inspired by cultural heritage,” in *Proceedings of the SIGCHI*, 2011, pp. 1919–1928.
- [7] M. Huang, S. Mehrotra, and F. Sparacino, “Shadow vision,” 1999.
- [8] I. B. K. Sudiatmika *et al.*, “Indonesian traditional shadow puppet image classification: A deep learning approach,” in *10th International Conference on Information Technology and Electrical Engineering*. IEEE, 2018, pp. 130–135.
- [9] I. B. K. Sudiatmika and I. G. A. A. S. Dewi, “Indonesian shadow puppet recognition using vgg-16 and cosine similarity,” *International Journal of Informatics and Computer Science*, vol. 5, no. 1, pp. 1–6, 2021.
- [10] A. Krizhevsky, “One weird trick for parallelizing convolutional neural networks,” *arXiv preprint arXiv:1404.5997*, 2014.
- [11] K. Simonyan and A. Zisserman, “Very deep convolutional networks for large-scale image recognition,” *arXiv preprint arXiv:1409.1556*, 2014.
- [12] K. He, G. Gkioxari, P. Dollár, and R. Girshick, “Mask r-cnn,” in *Proceedings of the ICCV*. IEEE, 2017, pp. 2961–2969.
- [13] A. G. Howard, M. Zhu, B. Chen, D. Kalenichenko, W. Wang, T. Weyand, M. Andreetto, and H. Adam, “Mobilennets: Efficient convolutional neural networks for mobile vision applications,” *arXiv 1704.04861*, 2017.
- [14] I. B. K. Sudiatmika, M. Artana, N. W. Utami, M. A. P. Putra, and E. G. A. Dewi, “Mask r-cnn for indonesian shadow puppet recognition and classification,” in *Journal of Physics: Conference Series*, vol. 1783, no. 1. IOP Publishing, 2021, p. 012032.
- [15] D. P. Prabowo, M. K. A. Nugraha, D. I. Ihya’Ulumuddin, R. A. Pramunendar, and S. Santosa, “Indonesian traditional shadow puppet classification using convolutional neural network,” in *International Seminar on Application for Technology of Information and Communication*. IEEE, 2021, pp. 1–5.
- [16] M. Brand, “Shadow puppetry,” in *Proceedings of the Seventh ICCV*, vol. 2. IEEE, 1999, pp. 1237–1244.
- [17] R. T. Collins, R. Gross, and J. Shi, “Silhouette-based human identification from body shape and gait,” in *Fifth international conference on automatic face gesture recognition*. IEEE, 2002, pp. 366–371.
- [18] T. B. Moeslund, A. Hilton, and V. Krüger, “A survey of advances in vision-based human motion capture and analysis,” *Computer vision and image understanding*, vol. 104, no. 2-3, pp. 90–126, 2006.

¹⁰MediaPipe — <https://developers.google.com/mediapipe>

¹¹Kinect for Windows — <https://learn.microsoft.com/en-us/windows/apps/design/devices/kinect-for-windows>

[19] A. Tsuji, K. Ushida, and Q. Chen, “Real time animation of 3d models with finger plays and hand shadow,” in *ACM International Conference on Interactive Surfaces and Spaces*. Association for Computing Machinery, 2018, p. 441–444.

[20] A. Tsuji, K. Ushida, S. Yamaguchi, and Q. Chen, “Real-time collaborative animation of 3d models with finger play and hand shadow,” in *Conference on Virtual Reality and 3D User Interfaces*. IEEE, 2019, pp. 1195–1196.

[21] A. Tsuji and K. Ushida, “Telecommunication using 3dcg avatars manipulated with finger plays and hand shadow,” in *10th Global Conference on Consumer Electronics*. IEEE, 2021, pp. 39–40.

[22] Z. Huang, V. K. Madaram, S. Albadrani, and T. V. Nguyen, “Shadow puppetry with robotic arms,” in *Proceedings of the 25th ACM international conference on Multimedia*, 2017, pp. 1251–1252.

[23] H. Zhang, Y. Song, Z. Chen, J. Cai, and K. Lu, “Chinese shadow puppetry with an interactive interface using the kinect sensor,” in *Proceedings of the ECCV Workshops and Demonstrations*. Springer, 2012, pp. 352–361.

[24] B. M. Carr and G. J. Brown, “Shadow puppetry using the kinect,” 2014.

[25] T.-H. Tsai and L.-C. Lee, “A study of using contactless gesture recognition on shadow puppet manipulation [j],” *ICIC express letters: an international journal of research and surveys*, vol. 7, no. 11, pp. 2317–2322, 2016.

[26] U. Güdükbay, F. Erol, and N. Erdogan, “Beyond tradition and modernity: digital shadow theater,” *Leonardo*, vol. 33, no. 4, pp. 264–265, 2000.

[27] S.-z. Gao, “On the digital development of the chinese shadow play art,” in *International Conference on Internet Technology and Applications*. IEEE, 2011, pp. 1–4.

[28] H. Liang, J. Chang, S. Deng, C. Chen, R. Tong, and J. Zhang, “Exploitation of novel multiplayer gesture-based interaction and virtual puppetry for digital storytelling to develop children’s narrative skills,” in *14th ACM SIGGRAPH*, 2015, pp. 63–72.

[29] Z. Yan, Z. Jia, Y. Chen, and H. Ding, “The interactive narration of chinese shadow play,” in *International Conference on Virtual Reality and Visualization*. IEEE, 2016, pp. 341–345.

[30] H. Liang, J. Chang, I. K. Kazmi, J. J. Zhang, and P. Jiao, “Hand gesture-based interactive puppetry system to assist storytelling for children,” *The Visual Computer*, vol. 33, pp. 517–531, 2017.

[31] Z. Tang, Y. Hu, W. Weng, L. Zhang, L. Zhang, and J. Ying, “An intelligent shadow play system with multi-dimensional interactive perception,” *International Journal of Human-Computer Interaction*, vol. 39, no. 6, pp. 1314–1326, 2023.

[32] N. Ma, X. Zhang, H.-T. Zheng, and J. Sun, “Shufflenet v2: Practical guidelines for efficient cnn architecture design,” in *ECCV*, 2018, pp. 116–131.

[33] A. Dosovitskiy, L. Beyer, A. Kolesnikov, D. Weissenborn, X. Zhai, T. Unterthiner, M. Dehghani, M. Minderer, G. Heigold, S. Gelly *et al.*, “An image is worth 16x16 words: Transformers for image recognition at scale,” *arXiv preprint arXiv:2010.11929*, 2020.

[34] F. N. Iandola, M. W. Moskewicz, K. Ashraf, S. Han, W. J. Dally, and K. Keutzer, “SqueezeNet: Alexnet-level accuracy with 50x fewer parameters and <1mb model size,” *ArXiv*, vol. abs/1602.07360, 2016.

[35] A. Howard, M. Sandler, G. Chu, L.-C. Chen, B. Chen, M. Tan, W. Wang, Y. Zhu, R. Pang, V. Vasudevan *et al.*, “Searching for mobilenetv3,” in *Proceedings of the IEEE/CVF ICCV*, 2019, pp. 1314–1324.

[36] Z. Liu, H. Mao, C.-Y. Wu, C. Feichtenhofer, T. Darrell, and S. Xie, “A convnet for the 2020s,” in *Proceedings of the IEEE/CVF CVPR*, 2022, pp. 11976–11986.

[37] M. Tan and Q. Le, “Efficientnet: Rethinking model scaling for convolutional neural networks,” in *ICML*. PMLR, 2019, pp. 6105–6114.

[38] S. Zagoruyko and N. Komodakis, “Wide residual networks,” *arXiv preprint arXiv:1605.07146*, 2016.

[39] M. Tan, B. Chen, R. Pang, V. Vasudevan, M. Sandler, A. Howard, and Q. V. Le, “Mnasnet: Platform-aware neural architecture search for mobile,” in *Proceedings of the IEEE/CVF CVPR*, 2019, pp. 2820–2828.

[40] M. Tan and Q. V. Le, “Efficientnetv2: Smaller models and faster training,” in *Proceedings of the ICML*. PMLR, 2021, pp. 10096–10106.

[41] M. Sandler, A. Howard, M. Zhu, A. Zhmoginov, and L.-C. Chen, “Mobilenetv2: Inverted residuals and linear bottlenecks,” in *Proceedings of the IEEE/CVF CVPR*, 2018, pp. 4510–4520.

[42] C. Szegedy, W. Liu, Y. Jia, P. Sermanet, S. Reed, D. Anguelov, D. Erhan, V. Vanhoucke, and A. Rabinovich, “Going deeper with convolutions,” in *Proceedings of the IEEE/CVF CVPR*, 2015, pp. 1–9.

[43] Z. Liu, H. Hu, Y. Lin, Z. Yao, Z. Xie, Y. Wei, J. Ning, Y. Cao, Z. Zhang, L. Dong *et al.*, “Swin transformer v2: Scaling up capacity and resolution,” in *Proceedings of the IEEE/CVF CVPR*, 2022, pp. 12009–12019.

[44] K. He, X. Zhang, S. Ren, and J. Sun, “Deep residual learning for image recognition,” in *Proceedings of the IEEE/CVF CVPR*, 2016, pp. 770–778.

[45] Z. Liu, Y. Lin, Y. Cao, H. Hu, Y. Wei, Z. Zhang, S. Lin, and B. Guo, “Swin transformer: Hierarchical vision transformer using shifted windows,” in *Proceedings of the IEEE/CVF CVPR*, 2021, pp. 10012–10022.

[46] Z. Tu, H. Talebi, H. Zhang, F. Yang, P. Milanfar, A. Bovik, and Y. Li, “Maxvit: Multi-axis vision transformer,” in *Proceedings of the ECCV: 17th European Conference*. Springer, 2022, pp. 459–479.

[47] I. Radosavovic, R. P. Kosaraju, R. Girshick, K. He, and P. Dollár, “Designing network design spaces,” in *IEEE/CVF CVPR*, 2020, pp. 10428–10436.

[48] G. Huang, Z. Liu, L. Van Der Maaten, and K. Q. Weinberger, “Densely connected convolutional networks,” in *IEEE/CVF CVPR*, 2017, pp. 4700–4708.

[49] S. Xie, R. Girshick, P. Dollár, Z. Tu, and K. He, “Aggregated residual transformations for deep neural networks,” in *IEEE/CVF CVPR*, 2017, pp. 1492–1500.

[50] C. Szegedy, V. Vanhoucke, S. Ioffe, J. Shlens, and Z. Wojna, “Rethinking the inception architecture for computer

vision,” in *IEEE/CVF CVPR*, 2016, pp. 2818–2826.

[51] J. Deng, W. Dong, R. Socher, L.-J. Li, K. Li, and L. Fei-Fei, “Imagenet: A large-scale hierarchical image database,” in *Proceedings of the IEEE/CVF CVPR*. IEEE, 2009, pp. 248–255.

[52] J. Maurício, I. Domingues, and J. Bernardino, “Comparing vision transformers and convolutional neural networks for image classification: A literature review,” *Applied Sciences*, vol. 13, no. 9, p. 5521, 2023.

[53] J. Kiefer and J. Wolfowitz, “Stochastic estimation of the maximum of a regression function,” *The Annals of Mathematical Statistics*, pp. 462–466, 1952.

[54] L. Van der Maaten and G. Hinton, “Visualizing data using t-sne.” *Journal of machine learning research*, vol. 9, no. 11, 2008.

[55] R. R. Selvaraju, M. Cogswell, A. Das, R. Vedantam, D. Parikh, and D. Batra, “Grad-cam: Visual explanations from deep networks via gradient-based localization,” in *Proceedings of the IEEE/CVF ICCV*, 2017, pp. 618–626.

[56] M. T. Ribeiro, S. Singh, and C. Guestrin, “Why should i trust you? explaining the predictions of any classifier,” in *22nd ACM SIGKDD*, 2016, pp. 1135–1144.

[57] K. Simonyan, A. Vedaldi, and A. Zisserman, “Deep inside convolutional networks: visualising image classification models and saliency maps,” in *Proceedings of the ICLR*, 2014.

[58] H. Mahmud, M. M. Morshed, and M. K. Hasan, “Quantized depth image and skeleton-based multimodal dynamic hand gesture recognition,” *The Visual Computer*, vol. 40, no. 1, p. 11-25, Jan. 2023.



Syed Rifat Raiyan was born in Agrabad, Chatogram, Bangladesh in 2001. His alma maters include PlaySchool, Milestone College, RAJUK Utara Model College, and Notre Dame College. He attained the Bachelor of Science (B.Sc.) degree with Honors from the Department of Computer Science and Engineering (CSE) at the Islamic University of Technology (IUT), Board Bazar, Gazipur-1704, Dhaka, in 2023.

He worked as an Industrial Trainee at Battery Low Interactive Ltd. in 2021. Since the 16th of August 2023, he has been working as a Lecturer in the Department of Computer Science and Engineering (CSE) at the Islamic University of Technology (IUT). He is currently affiliated with the Systems and Software Lab (SSL) research group of IUT. His research interests lie broadly in natural language processing, computer vision, and deep learning. His works have been published in the Findings of the Association for Computational Linguistics: ACL 2023 and in the Proceedings of the 61st Annual Meeting of the Association for Computational Linguistics (Volume 4: Student Research Workshop). His current endeavors revolve around projects concerning mathematical reasoning in language models, in-context learning for text classification, Bangla sentiment analysis, and image classification.

Mr. Raiyan has been a member of the Association for Computational Linguistics (ACL) since 2023. He was awarded the prestigious IUT Gold Medal in recognition of his stellar academic performance while pursuing his B.Sc. (Engg.) degree, in 2023.



Zibran Zarif Amio was born in Dulahazara, Cox’s Bazar, Bangladesh in 2000. His alma mater includes BIAM Laboratory School, Cox’s Bazar Govt. High School, and Dhaka Residential Model College. He attained the Bachelor of Science (B.Sc.) degree with First Class from the Department of Computer Science and Engineering (CSE) at the Islamic University of Technology (IUT), Board Bazar, Gazipur-1704, Dhaka, in 2023.

He worked as an Android Developer at BYDO Academy in 2020. He was an Industrial Trainee at Battery Low Interactive Ltd. in 2021. Since the 1st of June 2023, he has been working as the Chief Technology Officer at ReplyMind AI Ltd., Grameen Telecom Bhaban, Mirpur-1216, Dhaka. His work involves leading and developing Generative AI-enabled software solutions. His research interests lie broadly in natural language processing, computer vision, and deep learning. His current endeavors include Meta Business Automation with Large Language Models.



Sabbir Ahmed (Member’23, IEEE) is an Assistant Professor in the Dept of CSE at the Islamic University of Technology (IUT). He received a M.Sc. and B.Sc. (Gold medalist) in CSE from IUT, respectively, in the years 2022 and 2017. He is a member of the Computer Vision research group and his current research is in improving few-shot learning algorithms for image classification tasks. Besides, he has worked with different applications of deep learning in the field of computer vision, such as leaf disease classification, gait analysis, traffic sign detection, handwritten digit recognition, etc.